Control of impurities in PPV light-emitting devices

W. Brütting *, M. Meier, M. Herold, S. Karg, M. Schwoerer

Experimentalphysik II and Bayreuther Institut für Makromolekülforschung (BIMF), Universität Bayreuth, 95440 Bayreuth, Germany

Abstract

The influence of different substrates used for the fabrication of poly(p-phenylene vinylene) (PPV) light-emitting devices on the device characteristics is investigated with different experimental techniques, like current–voltage, brightness–voltage and capacitance–voltage measurements. Using thermally stimulated currents we determine the energetic depth and density of states created by doping of PPV during device fabrication. In devices prepared on indium–tin oxide (ITO) substrates doping with $InCl_3$ leads to states with a depth of about 0.15 eV and an ionized acceptor concentration in excess of 10^{16} cm^{-3}. These carriers are mobile and form a depletion layer of width 120 nm when a metal with low work function, like Al, is used as cathode. This doping is responsible for the observed Schottky diode behaviour in PPV devices on ITO. With fluorine-doped tin dioxide as transparent hole-injecting contact, trap energies increase slightly to 0.2 eV and the ionized acceptor concentration is lowered by a factor of five. The lower doping concentration leads to an increase of the depletion layer width to about 270 nm and thickness-dependent device characteristics. For PPV converted on gold no doping is detectable with capacitance–voltage measurements and thermally stimulated currents. Photoluminescence measurements show a significant quenching of fluorescence in PPV converted on ITO. We regard this as an important limiting factor for single and heterolayer devices with PPV as emissive material. © 1997 Elsevier Science S.A.

Keywords: Poly(p-phenylene vinylene); Light-emitting devices; Impurities

1. Introduction

Doping of conjugated polymers with the aim of replacing metals and the fabrication of organic electronic devices (e.g. diodes and transistors) was an important research area in the 1980s [1]. The discovery of electroluminescence (EL) in poly(p-phenylene vinylene) (PPV) by the Cambridge group in 1990 triggered intense research for optoelectronic devices based on conjugated polymers, combining the charge transport capabilities with optical properties like strong fluorescence in the visible [2]. Due to its good processability and high thermal stability PPV is still one of the most attractive materials for polymer light-emitting devices (LEDs) [3].

In many cases, the description of organic EL devices based on the concept of work functions, where the barriers for the injection of charge carriers are simply given by the difference of the metal work function and the energy levels (HOMO and LUMO) of the organic material, is not satisfactory. The presence of interfaces, e.g. formed by chemical reactions of the polymer with the electrodes, can influence the device characteristics significantly even in a simple single-layer device. Additionally, the assumption of a homogeneous volt-

age drop over the device is no longer valid in the presence of mobile carriers created by chemical doping. Instead of rigid bands one has to take into account band bending, which leads to a spatially non-uniform electric field distribution.

PPV prepared by the precursor route is particularly subjected to doping reactions since the thermal conversion of the precursor polymer to PPV is performed directly on the anode used for hole injection in LEDs. So, additionally to the known doping processes of conjugated polymers [1], there is the possibility of chemical reactions of the precursor polymer's leaving groups with the substrate, which can have strong influence on the electrical and optical properties of the devices. It is known from earlier investigations that the electrical conductivity of PPV prepared by the precursor route changes by several orders of magnitude when doped with electron acceptors [4]. Already the exposure to air increases the conductivity of pristine PPV films within seconds from 10^{-15} to more than 10^{-13} $(\Omega\ cm)^{-1}$ at room temperature. PPV prepared on an indium–tin oxide (ITO) substrate, a technique widely used for the preparation of polymer light-emitting devices, gives rise to an additional oxidation process through the reaction of indium (or more likely indium oxide) with the HCl leaving group during the thermal conversion of the precursor to the conjugated PPV. This doping reaction

* Corresponding author. E-mail: wolfgang.bruetting@uni-bayreuth.de

has been proven by depth profiling of ITO/PPV/Al devices with secondary ion mass spectrometry (SIMS), where enhanced Cl and In count rates were found throughout the whole PPV layer [5]. With scanning electron microscopy (SEM) using energy-dispersive X-ray analysis (EDX) the formation of $InCl_3$ has been detected at the ITO/PPV interface [6]. Since $InCl_3$ is known as an oxidizing agent, we believe that this compound is responsible for doping of PPV in the same way as has been shown earlier for $FeCl_3$ [7]. In ITO/PPV/metal LEDs this doping leads to both the formation of a Schottky barrier at the PPV/metal interface in the case of low work function metals, like Ca and Al, and an ohmic contact with good hole-injecting properties at the ITO/PPV interface. The existence of a Schottky contact in ITO/PPV/metal devices has been demonstrated by several experiments, e.g. photovoltaic experiments [8], photolumi-nescence (PL) quenching in an electric field [9], impedance spectroscopy [8,10,11] or X-ray photoelectron spectroscopy (XPS) measurements [12].

In this paper we will address the influence of different substrate materials on the electrical characteristics of PPV devices. Additionally we determine the concentration and energetic depth of dopants in PPV and discuss the consequences for PPV-based LEDs.

2. Experimental results and discussion

2.1. Current–voltage characteristics and electroluminescence

In Fig. 1 we compare current–voltage (I–V) and brightness–voltage characteristics of PPV devices fabricated on different anode materials (ITO, fluorine-doped tin dioxide (FTO) and gold (Au)). The PPV film thickness was about 450 nm and the active device area 0.25 cm^2. Except for the substrate, all devices were prepared as identical as possible;
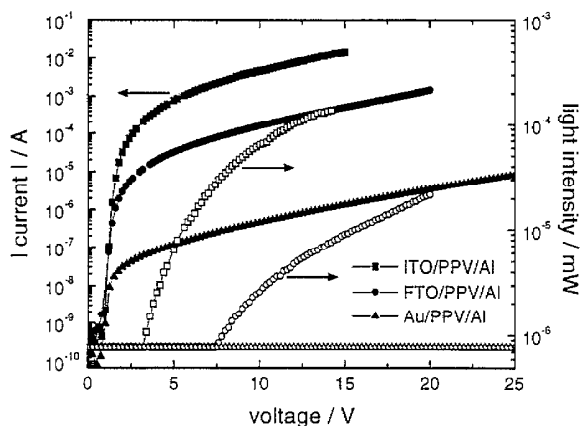

Fig. 1. I–V characteristics and light output of PPV devices fabricated on different substrate materials. The PPV thickness of all devices was about 450 nm and the active device area 0.25 cm^2. The flat line with a light intensity of 8×10^{-7} mW is the detection limit of our setup.

especially the evaporation of the Al cathode was performed simultaneously.

The I–V characteristics of ITO/PPV devices have been analysed in detail recently [10,13]; therefore, we only want to point out the significant differences to the other anode materials. The most striking difference among the three devices is the strong variation of the current in forward direction (Al biased negatively). All devices show rectification; however, the rectification ratio ρ_r at 5 V varies from almost 10^6 for ITO to only 10^2 for Au. The difference in current in reverse direction is less than two orders of magnitude.

In previous work by our group it has been shown that ITO/PPV/metal devices with low work function metals like Ca or Al are well described by a Schottky diode model, where the current is carried predominantly by holes and determined by a Schottky barrier at the PPV/metal interface [10,13]. The ITO/PPV contact is regarded as an ohmic contact with negligible injection barrier. Taking into account a serial resistance R_B of the PPV bulk, which is considerably larger than in conventional semiconductor Schottky diodes, the I–V characteristics in forward direction can be described well by the modified Shockley equation [14]:

$$j = j_S \left[\exp\left(\frac{q(V - IR_B)}{nkT}\right) - 1 \right] \qquad (1)$$

where n is the ideality factor and j_S the saturation current density.

The application of the model to the devices investigated here is meaningful for ITO and FTO as anode material. The exponential rise of the I–V characteristics immediately above 1 V and also the flattening at higher voltage can be well described within this model. Above 5 V, space charge limited currents lead to deviations from this description, which will not be discussed here. For Au it is questionable to use the Shockley equation since the exponential rise above 1 V is almost completely suppressed. In this case, however, one can get at least information about the bulk resistance of PPV.

We have fitted the I–V characteristics of the three devices with the modified Shockley Eq. (1) between 1 and 5 V in forward direction. The resulting parameters are listed in Table 1. The important parameter in this context is the PPV bulk resistance R_B which varies over five orders of magnitude: 4×10^2 Ω for ITO, 1.5×10^4 Ω for FTO and 7.1×10^7 Ω for Au. Taking the device geometry as given above, one can calculate the conductivity of the PPV bulk for the respective anode material. One yields values of 4.5×10^{-7} (Ω cm)$^{-1}$

Table 1
Device parameters [a] obtained from current–voltage characteristics shown in Fig. 1 by fitting the modified Shockley Eq. (1)

	j_S (A cm^{-2})	n	R_B (Ω)
ITO	2.1×10^{-13}	2.5	4×10^2
FTO	1.9×10^{-14}	2.5	1.5×10^4
Au	1.4×10^{-17}	2.8	7.1×10^7

[a] j_S: saturation current density, n: ideality factor, R_B: PPV bulk resistance.

for ITO, 1.2×10^{-8} $(\Omega$ cm$)^{-1}$ for FTO and 2.5×10^{-12} $(\Omega$ cm$)^{-1}$ for Au. This is not necessarily the ohmic conductivity of the material, since the device is in the carrier injection regime and not in thermodynamic equilibrium. The data for Au are in good agreement with published d.c. conductivity measurements performed on free-standing PPV films [15]; thus, for the other materials the calculation should at least give an estimate of the order of magnitude. The drastic change in conductivity from Au to ITO is clear evidence that the fabrication of PPV devices on ITO substrates leads to doping of the polymer. With FTO as anode material, which is expected to be chemically more inert, the degree of doping must be less compared to ITO.

The open symbols in Fig. 1 show the EL light output of the three devices measured simultaneously with the I–V characteristics. For ITO we observe EL for a bias voltage $V > 3$ V, the FTO device has an onset voltage of about 7.5 V, and for the Au device no EL is detectable for voltages up to 25 V at this thickness.

In previous work we have shown that the onset voltage for ITO/PPV devices with Ca or Al as cathode can be as low as 1.5 V and it is essentially independent of the PPV thickness between 200 and 800 nm [10,13]. For FTO devices we observe a strong thickness dependence of the onset voltage, but not a linear relationship, which indicates that carrier injection is not simply governed by the electric field.

2.2. Capacitance–voltage spectroscopy

More quantitative information about doping concentration in these devices can be obtained from capacitance–voltage spectroscopy. Fig. 2 shows the bias-voltage-dependent capacitance of the three devices. For ITO devices we observe a strong voltage dependence caused by mobile charge carriers in the material. The capacitance peaks at about 1.3 V, which is equivalent to the diffusion voltage of the Schottky barrier, necessary to obtain flat band condition. In the case of FTO the variation of the capacitance with bias is much smaller, suggesting a lower concentration of mobile carriers. In Au
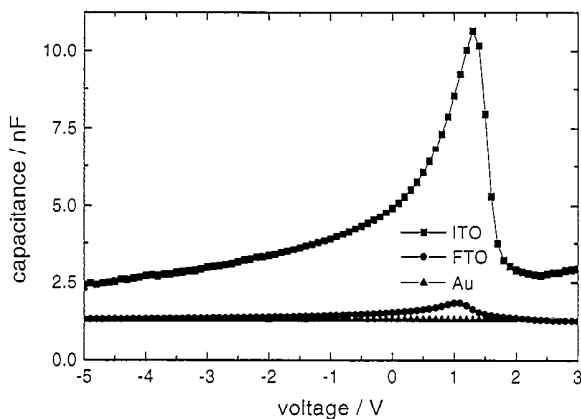
devices the capacitance is virtually voltage independent and equivalent to the geometrical capacitance of a PPV film with a dielectric constant of $\epsilon \approx 3$.

Assuming an abrupt junction, the bias-dependent capacitance and depletion layer width of a Schottky junction are given by [14]

$$C_J = A \left[\frac{q \epsilon_0 \epsilon N_A}{2(V_D - V)} \right]^{1/2} ;$$

$$w = \left[\frac{2 \epsilon_0 \epsilon (V_D - V)}{q N_A} \right]^{1/2} \qquad (2)$$

where N_A is the ionized acceptor concentration and V_D the diffusion voltage. Thus, a linear plot of $1/C_J^2$ versus voltage in reverse direction should give a straight line with a slope proportional to N_A^{-1}.

The data of Fig. 2 have been evaluated with Eqs. (2) yielding parameters listed in Table 2. The data clearly show that the concentration of ionized dopants in the three devices decreases by a factor of five from ITO to FTO and at least by another factor of five from FTO to Au. Thus, the width of the depletion layer at zero bias calculated within this model increases from 120 nm for ITO to 270 nm for FTO, which is already more than half the device thickness (450 nm). Therefore, it is reasonable that with FTO substrates the device characteristics are no longer thickness independent for a PPV thickness between 200 and 800 nm (as is the case with ITO). Additionally, the FTO device has a larger bulk resistance, which also causes a considerably higher voltage drop at the PPV bulk, and the injection barrier for holes is also probably larger.

2.3. Thermally stimulated currents

In order to get more information about the dopant species and the influence on charge transport in PPV, we have performed thermally stimulated current (TSC) measurements, which is a classical method for the determination of the energetic depth and density of trap states in inorganic semiconductors as well as organic materials [16,17]. In the experiment the sample is cooled to an initial temperature of about 10 K. At this temperature the traps are filled by applying current for a certain period of time. Finally, while the sample is heated up to room temperature at a constant heating rate of several K min^{-1} the discharge current without bias (short-circuit operation) is recorded as a function of temperature. When charge carriers are thermally detrapped, peaks in the TSC spectra occur. From the position and form of these TSC maxima the energetic depth and the concentration of trap states can be determined. In this contribution we discuss the results obtained on PPV LEDs only briefly; a detailed survey will be given in a forthcoming paper [18].

Fig. 3 shows a comparison of TSC spectra of ITO/PPV/Al and Au/PPV/Al devices in the temperature range from 10 to 200 K. Both samples had a PPV layer thickness of about 600 nm and the trap filling was performed identically, passing

Fig. 2. Capacitance–voltage dependence of PPV devices fabricated on different substrate materials. Devices were taken from the same batch as in Fig. 1.

Table 2

Device parameters [a] obtained from capacitance–voltage measurements shown in Fig. 2 by using Eqs. (2)

	N_A (cm^{-3})	V_D (V)	w (nm)
ITO	2.3×10^{16}	1.3	120
FTO	5×10^{15}	1.1	270
Au	$< 10^{15}$		

[a] N_A: ionized acceptor concentration, V_D: diffusion voltage, w: depletion layer width at zero bias.
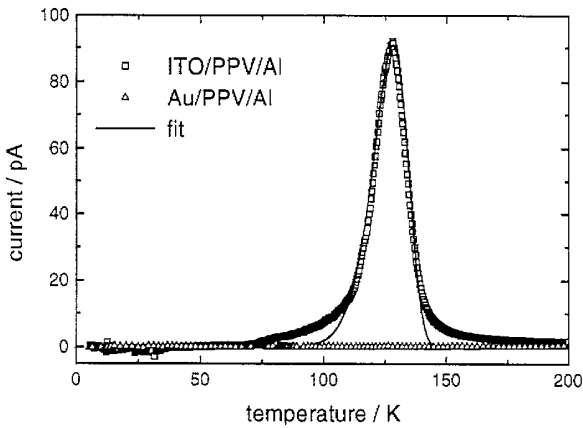

Fig. 3. Thermally stimulated currents of PPV devices fabricated on ITO and Au substrates. The PPV thickness of both devices was about 600 nm and the active device area 0.25 cm^2.

a current of 10 μA at 10 K for 5 min through the device. The curves were recorded at a heating rate of about 5 K min^{-1}. While there is no TSC signal detectable within our experimental resolution (10^{-13} A) when Au is used as anode, the sample with ITO clearly shows a peak at about 128 K. Thus, the elimination of PPV on ITO substrates creates at least one trap state detectable with TSC.

A current peak in the TSC spectrum for a trap species with discrete energy E_t (relative to the valence band for a hole conductor) is of the following form [17]:

$$I(T) \propto \exp\left[-\frac{E_t}{kT} - \alpha \int_{T_0}^{T} \beta \exp\left(-\frac{E_t}{kT'} \right) dT' \right] \qquad (3)$$

Following a method proposed by Cowell and Woods [19] the integral can be approximated by the first term of a series expansion, leading to an analytical expression for $I(T)$. α and β are parameters depending on the retrapping kinetics and the attempt-to-escape frequency, which are not known for PPV. Nevertheless, the formula can be used for determining the trap energy E_t. The released charge is obtained by integrating the TSC spectrum over time. With the sample geometry this then gives the density of released carriers.

The TSC spectrum for ITO shown in Fig. 3 has been evaluated assuming one discrete trap energy. From the fit shown in the figure a trap depth of $E_t = 0.18$ eV is obtained. There are deviations at the bottom of the peak, which can be attributed to either a distribution of trap energies or, more likely,

to a second broader peak superimposed. For the latter case we have obtained a second trap energy of about 0.05 eV by fitting the experimental data with a superposition of two TSC peaks. The integral of the curve yields a trap density of $N_t \approx 10^{16}$ cm^{-3}. For the FTO substrate (not shown in Fig. 3) we find qualitatively similar results with one major peak at 165 K with $E_t \approx 0.2$ eV and a second smaller peak at 100 K with $E_t \approx 0.02$ eV. The total trap density of the two peaks is with the same trap filling conditions about a factor of three lower than with ITO. The trap densities obtained by TSC are in good agreement with the ionized acceptor concentrations obtained from capacitance–voltage analysis given in Table 2. Thus, we can clearly identify the doping of PPV on ITO (and less effective on FTO) as the origin of shallow traps with energies lower than 0.2 eV.

In the temperature range above 200 K we find additional TSC peaks independent of the substrate used. The depth of these trap species is between 0.6 and 0.9 eV. Their density can be reduced by applying vacuum to the devices or increased by exposure to oxygen, indicating a reversible doping process by oxygen, which could be assigned to the observations in d.c. conductivity measurements as described in Section 1 [4]. A detailed investigation of these peaks is in preparation [18].

2.4. Implications for light-emitting devices

For efficient organic EL devices a series of different physical processes have to be optimized: injection and transport of carriers of both polarity, formation of excitons and their radiative recombination. Our investigations show that PPV converted on ITO is a well-suited material for efficient injection of holes, although from the concept of work functions there should be a considerable barrier between ITO ($\Phi \approx 4.3$ eV) and the ionization potential of PPV ($I_P \approx 5.0$ eV). However, the doping reaction by InCl$_3$ formed during thermal conversion leads to a highly p-doped interface region, which can be regarded as an ohmic contact — in analogy to inorganic semiconductor devices. The hole mobilities in PPV derived from space charge limited currents in excess of 10^{-5} cm^2 V^{-1} s^{-1} are also acceptable for many device applications [10,13]. Doping of the PPV bulk leads to the formation of a Schottky contact with low work function cathode materials. With its spatially inhomogenous field distribution this contact enables electron injection at low voltages. Additionally, it is responsible for device characteristics almost independent of the PPV bulk thickness. Thus, leakage currents in these devices caused by considerable surface roughness of the substrate materials (typically 10 to 50 nm) or by dust particles can be overcome by using larger film thicknesses.

The most important drawback of ITO/PPV devices is their low EL quantum efficiency of 0.01% (external) or less, depending on the cathode material, which is a consequence of the large excess hole current in the Schottky diode as a majority carrier device. It has been shown that charge balance can be improved considerably by using a second organic layer with hole-blocking and electron-conducting properties

Table 3

Comparison of ITO/PPV single-layer and heterolayer LEDs with a starburst oxadiazole [24] and Alq₃ as electron transport layer and a Mg:Ag (10:1) cathode [a]

	V (V)	L (cd m^{-2})	η_{ext} (%)	η_L (lm W^{-1})
ITO/PPV/Mg:Ag	10	30	0.005	0.003
ITO/PPV/Oxd/Mg:Ag	15–20	500	0.1	0.025
ITO/PPV/Alq₃/Mg:Ag	15–20	2500	0.5	0.25

[a] Layer thickness: PPV 100 nm, oxadiazole 30 nm, Alq₃ 50 nm, Mg:Ag 100 nm; V: operating voltage, L: radiance, η_{ext}: external quantum efficiency, η_L: power efficiency.
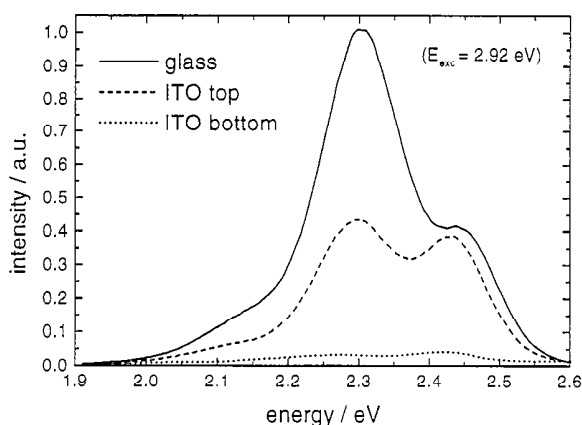

Fig. 4. PL spectra of PPV films (with a thickness of 600 nm) converted on ITO and glass. Films were pulled off the substrate after conversion and spectra were taken from both sides of the film. All spectra are scaled with the same factor.

[20,21] or in metal/insulator/polymer structures with an additional interfacial oxide layer [22]. With our devices we have found that the usage of oxadiazole polymers and starburst molecules increases the external quantum efficiency to about 0.1% (see also Table 3).

As in these heterolayer devices PPV is still the emitting material, one also has to look at the effects of doping on the fluorescence properties of PPV. Fig. 4 shows the comparison of PL spectra of a 600 nm thick PPV film converted on glass and ITO. The spectra in Fig. 4 can be compared quantitatively since they are all measured in the same geometry and normalized with the same scaling factor. After conversion the films were pulled off the substrate and PL spectra were taken from both sides of the film. Owing to the high absorption coefficient of PPV (3×10^5 cm^{-1} at the excitation energy of $E = 2.92$ eV) the penetration depth (drop of intensity to $1/e$) of the incident light is 33 nm.

Therefore, this experiment probes fluorescence only within the first 100 nm of the PPV film.

In the case of glass, both sides of the film exhibit the same PL spectra (thus only one curve is plotted). On PPV films prepared in this way we have measured independently absolute PL efficiencies of about 15% using an integrating sphere as described by Greenham et al. [23]. With ITO as substrate the PL intensity is quenched at the top of the film by about a factor of two; at the bottom the quenching is more than 20. PPV films converted on FTO or Au substrates show essen-

tially the same PL spectrum and intensity as the film converted on glass.

This clearly demonstrates that the doping of PPV films converted on ITO significantly reduces the PL efficiency. The quenching is more than one order of magnitude at the ITO/PPV interface, but even at the top of a 600 nm thick film PL efficiency is significantly reduced. Although the doping profile is not exactly known and the spatial distribution and concentration of dopants created during the elimination reaction may probably depend on the film thickness and conversion conditions, it has to be expected that in PPV films with a thickness of 100 to 200 nm, typically used for single-layer and heterolayer LEDs, one has significant PL quenching effects, which reduce the overall EL efficiency.

Consequently, it is not favourable to use PPV converted on ITO as emission layer in single-layer or heterolayer devices. This is manifested from the data in Table 3, where we compare the performance of devices having PPV as emitter in a single-layer device, a double-layer device with starburst oxadiazole as electron transport layer and a double-layer device with 8-hydroxyquinoline-aluminium (Alq₃) as electron transport material. The data in the table show that at the same operating voltage for the Alq₃ devices we measure brightness and efficiency five times higher as compared to the oxadiazole device. In the case of Alq₃ the EL emission spectra show that the emission originates essentially from Alq₃ and not from PPV. Regarding the electron injection (LUMO energy) and transport (electron mobility) properties, the data for Alq₃ and oxadiazoles are comparable [24,25]. Thus, the lower efficiency and brightness in PPV/oxadiazole devices reflect the important effect of PL quenching in PPV converted on ITO substrates.

3. Conclusions

Our investigations show that LEDs from precursor PPV are subjected to doping processes caused by the substrate used for device fabrication. The resulting device characteristics strongly depend on the doping concentration in PPV. An ionized acceptor concentration of more than 10^{16} cm^{-3} in ITO devices is sufficient for the formation of a Schottky contact at the PPV/cathode interface, which determines the device characteristics. The doping by InCl₃, formed by the reaction of ITO with the precursor leaving group HCl, leads to a significant PL quenching, which reduces EL quantum efficiency also in heterolayer devices with PPV as emission

layer. Hence, for efficient LEDs we propose to use precursor PPV with less aggressive leaving groups or additional highly fluorescent polymers on PPV.

With FTO as anode a reduction of the doping concentration to some 10^{15} cm^{-3} already leads to field-dependent — non-Schottky type — device characteristics. Since there is no measurable PL quenching with FTO, we regard this chemically more inert material as a promising candidate for a transparent conducting anode for polymer LEDs based on precursor PPV. Further investigations are in progress in order to get a sufficient device characterization using this material.

References

[1] T. Skotheim, Handbook of Conducting Polymers, Marcel Dekker, New York, 1986.

[2] J. Burroughes, D.D.C. Bradley, A.R. Brown, R.N. Marks, K. Mackay, R.H. Friend, P.L. Burn and A.B. Holmes, Nature, 347 (1990) 539.

[3] ICSM '96 Conf. Proc., Synth. Met., 84–86 (1997).

[4] I. Murase, T. Ohnishi, T. Noguchi and M. Hirooka, Polym. Commun., 25 (1984) 327.

[5] G. Sauer, M. Kilo, M. Hund, A. Wokaun, S. Karg, M. Meier, W. Rieß, M. Schwoerer, H. Suzuki, J. Simmerer, H. Meyer and D. Haarer, Fresenius Z. Analyt. Chem., 353 (1996) 642.

[6] M. Herold, J. Gmeiner, C. Drummer and M. Schwoerer, J. Mater. Sci., (1997) submitted for publication.

[7] R. Mertens, P. Nagels, R. Callaerts, M. Van Roy, J. Briers and H.J. Geise, Synth. Met., 51 (1992) 55.

[8] W. Rieß, S. Karg, M. Meier, V. Dyakonov and M. Schwoerer, J. Lumin., 60–61 (1994) 960.

[9] U. Lemmer, S. Karg, M. Scheidler, M. Deussen, W. Rieß, B. Cleve, P. Thomas, H. Bässler, M. Schwoerer and E.O. Göbel, Synth. Met., 67 (1994) 169.

[10] W. Rieß, in S. Miyata and H. Nalwa (eds.), Organic Electroluminescent Materials and Devices, Gordon and Breach, London, 1996.

[11] M. Meier, S. Karg and W. Rieß, J. Appl. Phys., 82 (1997) 1961.

[12] E. Ettedugi, H. Razafitrimo, K.T. Park, Y. Gao and B.R. Hsieh, Surf. Interface Anal., 23 (1995) 89.

[13] S. Karg, M. Meier and W. Rieß, J. Appl. Phys., 82 (1997) 1951.

[14] S. Sze, Physics of Semiconductor Devices, Wiley, New York, 1981.

[15] J. Gmeiner, S. Karg, M. Meier, W. Rieß, P. Strohriegl and M. Schwoerer, Acta Polym., 4 (1993) 201.

[16] M. Pope and C.E. Swenberg, Electronic Processes in Organic Crystals, Clarendon Press, Oxford, 1982.

[17] K. Kao and W. Hwang, Electrical Transport in Solids, Pergamon, Oxford, 1981.

[18] M. Meier, S. Karg, K. Zuleeg, W. Brütting and M. Schwoerer, J. Appl. Phys., submitted for publication.

[19] T. Cowell and J. Woods, Br. J. Appl. Phys., 18 (1967) 1045.

[20] A. Brown, D.D.C. Bradley, J.H. Burroughes, R.H. Friend, N.C. Greenham, P.L. Burn, A.B. Holmes and A. Kraft, Appl. Phys. Lett., 61 (1992) 2793.

[21] E. Buchwald, M. Meier, S. Karg, P. Pösch, H.-W. Schmidt, P. Strohriegl, W. Rieß and M. Schwoerer, Adv. Mater., 7 (1995) 839.

[22] M. Meier, E. Buchwald, S. Karg, M. Cölle, J. Gmeiner, W. Rieß and M. Schwoerer, Mol. Cryst. Liq. Cryst., 283 (1996) 197.

[23] N. Greenham, I.D.W. Samuel, G.R. Hayes, R.T. Philips, Y.A.R.R. Kessener, S.C. Moratti, A.B. Holmes and R.H. Friend, Chem. Phys. Lett., 241 (1995) 89.

[24] J. Bettenhausen, P. Strohriegl, W. Brütting, H. Tokuhisa and T. Tsutsui, J. Appl. Phys., (1997) submitted for publication.

[25] R. Kepler, P.M. Beeson, S.J. Jakobs, R.A. Anderson, M.B. Sinclair, V.S. Valencia and P.A. Cahill, Appl. Phys. Lett., 66 (1995) 3618.